XLI CILAMCE
XLI Ibero-Latin American Congress on Computational Methods in Engineering
16-19 November, 2020 FOZ DO IGUAÇU PARANÁ - BRAZIL

NUMERICAL ANALYSIS OF THE BEHAVIOR OF CONCRETE COLUMNS CONFINED WITH CFRP USING THE CONSTITUTIVE MODEL *CONCRETE DAMAGED PLASTICITY*

Matheus de Santana Santos[1], Tereza Denyse Pereira de Araújo[1]

[1]*Department of Structural Engineering and Civil Construction, Federal University of Ceará*
Pici Campus, Block 728, Zip code 60455-760, Fortaleza/Ceará, Brazil
matheusdesantanaeng19@gmail.com, denyse@ufc.com.br

Abstract. The use of carbon fiber reinforced polymers (CFRP) in the reinforcement of concrete structures was consolidated in civil construction due to its excellent mechanical properties and low specific weight. In this context, this article aims to present numerical simulations in finite elements of columns reinforced externally to the CFRP, submitted to centralized compression. The simulations were developed considering the physical non-linearity of the concrete through the constitutive model *Concrete Damaged Plasticity* (CDP), based on plasticity and damage to the material. The numerical models were calibrated with data from experimental tests and indicated good compatibility of forces and axial displacements. The distribution of the compression stresses indicated that for the case of centered force the circular columns present uniform confinement, while in the prismatic columns the confinement is concentrated close to the rounded corners. The reinforcement efficiency in the resistance gain for different column cross sections was proven.

Keywords: Column reinforcement, Carbon fiber reinforced polymers, Confinement, Concrete damaged plasticity, Numerical analysis.

1 Introduction

In the last decades, there has been a considerable growth in research related to the repair and reinforcement of concrete structures, in order to discover new materials and improve the execution techniques. With regard to the reinforcement of concrete structures, in the midst of several existing techniques, the use of composite materials formed by the combination of a polymeric matrix and a reinforcement material made of fibers has been expanding and becoming an economically viable and technical quality compared to conventional methods.

Among the types of composite materials, Carbon Fiber Reinforced Polymers (CFRP) are considered by many authors [1–6] as an efficient option and widely used today for the reinforcement of structures, mainly due to its non-corrosive essence, low specific weight, high resistance tensile strength, high modulus of elasticity, easy handling and simple application.

According to ACI [7], the oldest technique for applying CFRP in reinforcing concrete structures was performed using the EB method (*Externally Bonded*), which consists of the external adhesion of CFRP sheets, fabrics or laminates on the concrete surface and can be applied to a variety of elements. The columns are essential elements to guarantee the stability of portico, since their collapse generally causes a global rupture of the structure, it is essential to explore the advantages offered by reinforcement systems that complement their resistant capacity.

The CFRP reinforcement technique has as its basic principle the confinement mechanism, which acts by increasing the strength of the concrete by preventing its lateral expansion, without there being a significant increase in the cross sectional area of the column. Thus, this article seeks to evaluate through numerical analyzes the increase in the resistant capacity of concrete columns with unidirectional CFRP blankets. The numerical simulations were performed at ABAQUS using the constitutive *Concrete Damaged Plasticity* (CDP) model, as a way of representing the physical nonlinearity of the concrete. CDP validation was performed by comparing the results obtained with experimental works.

2 Reinforcement of concrete columns

Traditional column reinforcement techniques (high performance concrete jacketing, external bonding of steel sheets, etc.) have disadvantages such as sudden changes in the cross sections of the parts or manifest sensitivity to atmospheric agents. In contrast, the techniques that use fiber composite materials do not alter the geometry of the columns due to their low thickness and the material used has greater durability than conventional concrete itself.

2.1 Confinement mechanism

According to Oliveira and Carrazedo [8] when a concrete pillar is compressed axially, due to the effect of the Poisson's ratio, axial (shortening) and transverse (lateral expansion) deformations occur proportionally and simultaneously. As the level of loading increases, there is the formation of micro cracks between the aggregates and the cement paste, generating large increments of transverse strains for small increases in longitudinal strains. The grouping of these micro cracks gives rise to the appearance of crack frames, which can lead to the failure of the structural element.

In this way, Sudano [9] reveals that the principle of column reinforcement consists in restricting the lateral expansion of the element, reducing the appearance of cracks along the concrete and delaying its rupture. Therefore, confinement presents itself as an adequate reinforcement technique, as it restricts the transverse deformation of compressed parts and still allows an increase in the strength of the concrete through the insertion of lateral pressures, as shown in Fig. 1.

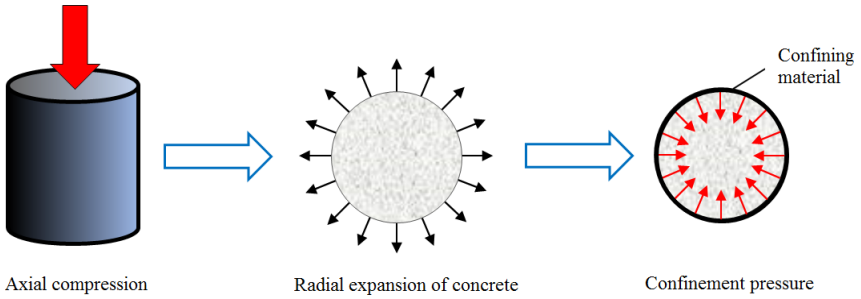

Figure 1. Concrete confinement mechanism

In order to obtain an adequate confinement of the concrete in columns, it is necessary that it be surrounded by materials that present good tensile strength, arranged in order to restrict the increase in transverse deformations.

2.2 Carbon fiber reinforced polymers

Fiber-reinforced polymers are composite materials formed by the union of high-strength fibers wrapped in a polymeric resin matrix. Fibers are responsible for providing most of the strength and stiffness of the composite, being considered its main constituent. In turn, the polymeric matrix ensures the transfer of stresses between the fibers by completely wrapping them, in addition to providing durability to the material, as it protects it from damages arising from manufacture and wear and tear throughout its useful life [10].

The preference for carbon fibers is justified by the high modulus of elasticity and high resistance. In addition, carbon fibers are resistant to any type of chemical attack, since carbon is an inert material, has good fatigue behavior, thermal and rheological variation, and low specific weight. As disadvantages, Carneiro [11] states that carbon fibers have a high cost, low resistance to impact loads and have high electrical conductivity.

3 Constitutive model

A constitutive model represents how the unit stresses and strains produced within a material are related. This relationship must be based on a determined number of parameters derived from the mechanical properties of the analyzed material.

The vast majority of constitutive models are based on the Theory of Plasticity or the Mechanics of Continuous Damage. Recently, a model of continuous damage coupled with plasticity for concrete known as *Concrete*

Damaged Plasticity (CDP) and available at Abaqus was developed.

3.1 Concrete Damaged Plasticity (CDP)

The CDP assumes that the nonlinear behavior of the concrete is the micro-cracking process, responsible for the loss of stiffness and plasticization, so that the total strain ε is given by the sum of a recoverable portion ε^{el} and an irreversible portion ε^{pl}:

$$\varepsilon = \varepsilon^{el} + \varepsilon^{pl}. \tag{1}$$

Considering the process of irreversible damage, the nominal stress σ is expressed by eq. (2):

$$\sigma = (1-d)D_0^{el} : (\varepsilon - \varepsilon^{pl}), \tag{2}$$

where d is the one-dimensional damage variable, responsible for material degradation, and D_0^{el} is the elastic constitutive tensor of intact material. Therefore, the constitutive model of plasticity and damage is based on the following stress-strain relationship:

$$\sigma = (1-d)\overline{\sigma} \rightarrow \sigma = (1-d_t)\overline{\sigma}_t + (1-d_c)\overline{\sigma}_c, \tag{3}$$

where $\overline{\sigma}$ represents the effective stress, and d_t and d_c represent the scalar variables of tensile and compression damage, respectively, ranging from 0 (material without damage) to 1 (material totally damaged). In this model, the existence of two types of failure mechanisms is admitted: rupture by traction or crushing of concrete by compression. The evolution of the failure is controlled by two hardening variables, represented by the plastic deformations under compression $\varepsilon_c^{pl,h}$ and under tensile $\varepsilon_t^{pl,h}$:

$$\varepsilon^{pl,h} = \begin{bmatrix} \varepsilon_t^{pl,h} \\ \\ \varepsilon_c^{pl,h} \end{bmatrix}; \varepsilon^{pl} = h\left(\varepsilon^{pl}, \overline{\sigma}\right) \cdot \dot{\varepsilon}^{pl}, \tag{4}$$

where h is a vector that defines a direction of hardening and $\dot{\varepsilon}^{pl}$ is a vector of eigenvalues of the plastic strain tensor.

The behavior of concrete is explained by the assumption that the plastic damage uses the yield function $f(\varepsilon^{pl,h}, \overline{\sigma})$, which represents a runoff surface in the stress space, to determine material damage or failure states [12].

In the CDP, the plastic deformation flow law is defined by eq. (5) and is non-associative, that is, the yield function and the plastic potential G do not match. The plastic potential is defined in the effective stress space.

$$\dot{\varepsilon}^{pl} = \frac{\delta G(\overline{\sigma})}{\delta \overline{\sigma}}. \tag{5}$$

The uniaxial compression and tensile responses of the concrete in relation to the damaged plasticity model are expressed by the eqs. (6) and (7), respectively:

$$\sigma_c = (1-d_c)E_0(\varepsilon_c - \varepsilon_c^{pl,h}), \tag{6}$$

$$\sigma_t = (1-d_t)E_0(\varepsilon_t - \varepsilon_t^{pl,h}). \tag{7}$$

Given the uniaxial nominal stresses, the respective uniaxial effective stresses $\overline{\sigma}_c$ and $\overline{\sigma}_t$ are:

$$\overline{\sigma}_c = \frac{\sigma_c}{(1-d_c)} = E_0(\varepsilon_c - \varepsilon_c^{pl,h}), \tag{8}$$

$$\overline{\sigma}_t = \frac{\sigma_t}{(1-d_t)} = E_0(\varepsilon_t - \varepsilon_t^{pl,h}), \tag{9}$$

where the compression deformation ε_c is equivalent to $(\varepsilon_c^{el} + \varepsilon_c^{pl,h})$ and the tensile deformation ε_t is equivalent to $(\varepsilon_t^{el} + \varepsilon_t^{pl,h})$.

4 Numerical simulations

In this article, columns subjected to centered compression were modeled from data from experimental tests performed by Carrazedo [13]. All the columns analyzed are 45 cm high, varying between them the cross section (square S, rectangular R and circular C), the rounding radius of the corners (r) and the number of layers of CFRP. The properties of the concrete and the CFRP blanket are shown in Table 1. As the type of CFRP adopted by Carrazedo [13] is a unidirectional blanket, only the properties of the fibers were pointed out, suppressing the properties of the resin and considering the 0° orientation for the reinforcement.

Table 1. Material properties used in the simulations

Concrete		CFRP (carbon fibers)	
Modulus of elasticity (E_0)	28500 MPa	Modulus of elasticity (E_f)	218950 MPa
Compressive strength (f_c)	36.4 MPa	Tensile strength (f_f)	2757 MPa
Tensile strength (f_t)	3.33 MPa	Ultimate tensile deformation (ε_{tu})	1.3 x 10^{-3}
Peak compression strain (ε_c)	0.003	Equivalent thickness (t)	0.17 mm
Fracture energy (G_f) [14]	0.134 N/mm		

The finite element numerical simulation was developed using the Abaqus V.14 software. The concrete was modeled using the three-dimensional solid element C3D8R (Fig.2a), which has 8 nodes, three degrees of freedom in each node and reduced integration. To model the CFRP blanket, the S4R shell element (Fig.2b) was used, which has 4 nodes, 6 degrees of freedom in each node and reduced integration. The dimensions of the finite elements were agreed to not exceed the value of 8 mm. The condition of total adherence between the materials was adopted through the command *tie*. The boundary conditions of the static test were represented considering the lower end of the abutment and the upper end coupled to a reference point that allows vertical displacement (Fig.2c). The load application occurred directly on the reference point.

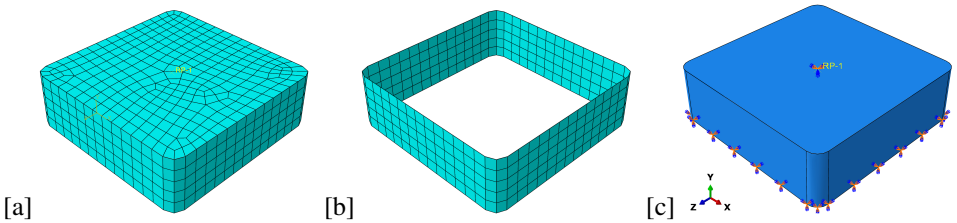

Figure 2. Boundary conditions and finite element meshes (small scale model)

Table 2 presents the standard Abaqus input values for all parameters of the CDP model, with the expansion angle ψ and the viscosity parameter μ calibrated according to the experimental data, guaranteeing the quality of the numerical models. For this work, the values of ψ = 45° and μ = 0.0001 presented satisfactory results.

Table 2. CDP model input parameters

Dilation angle (ψ)	Eccentricity (ϵ)	f_{b0}/f_{c0}	K	Viscosity parameter (μ)
calibrate	0.1	1.16	0.667	*calibrate*

In addition, it was necessary to define the uniaxial behavior of the concrete for compression loading (Fig.3a), the fracture energy (Table 1) as a simplified way to consider the effect of traction, and the evolution of the damage when subject to compression (Fig.3b) or traction (Fig.3c) loads. The stress-strain curve was constructed from the formulation proposed by Mansur et al. [15], the fracture energy was calculated according to CEB-FIP [14] and the damage evolution behavior was based on the work published by Birtel and Mark [16].

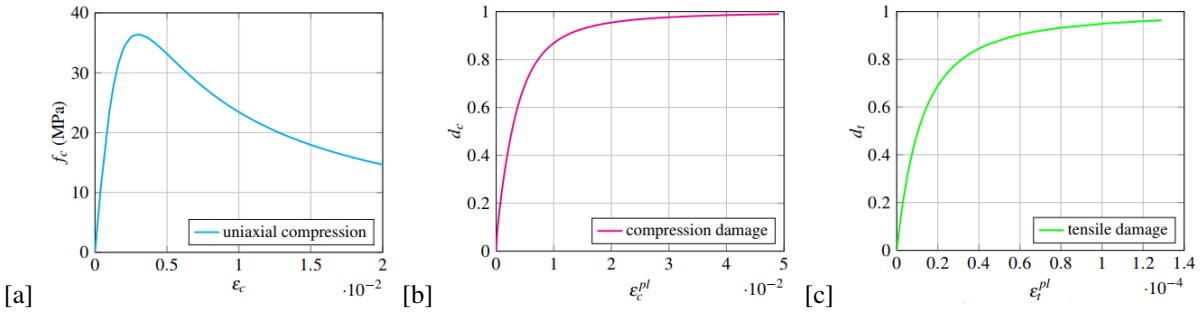

Figure 3. Concrete behavior to uniaxial compression and damage evolution

The results achieved were obtained by applying the non-linear resolution method *Static General* from Abaqus. For a total time equal to 1, the values used for the automatic control of the incremental scheme were 0.00001 for the minimum increment, 0.01 for the initial increment and 0.1 for the maximum increment.

5 Results and discussion

Table 3 shows the values of the force F_c and displacement δ_c axial peak in compression, comparing the numerical results with the experimental results; and in Fig. 4 the force-displacement curves of the numerical models are shown in comparison with the curves obtained by Carrazedo [13]. In the legends, the nomenclature of the columns is represented by the type of cross section (first letter), number of layers of CFRP (first number) and rounding radius of the corners (third number).

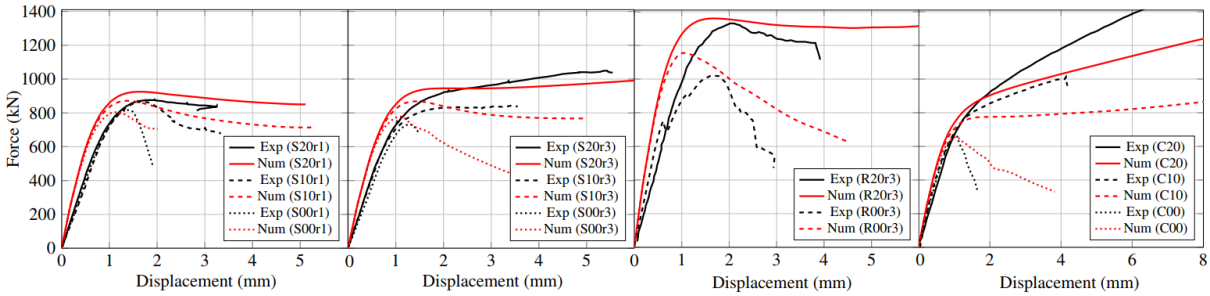

Figure 4. Comparison between numerical and experimental force-displacement curves

It is possible to highlight a good approximation between numerical and experimental curves, in which it is possible to verify that the numerical models are able to recognize deformations and increase stresses in reinforced columns, in addition to representing the ascending or descending post-peak of each analyzed column. As an average of the ratios between the experimental and numerical results, 0.99 for the peak force and 1.08 for the peak displacement were obtained.

Table 3. Comparison between experimental and numerical results of peak compression

Pillar	$F_{c,exp}$ (kN)	$F_{c,num}$ (kN)	/ (a)	$\delta_{c,exp}$ (mm)	$\delta_{c,num}$ (mm)	/	Pillar	$F_{c,exp}$ (kN)	$F_{c,num}$ (kN)	/	$\delta_{c,exp}$ (mm)	$\delta_{c,num}$ (mm)	/
S00r1	815	804.6	0.99	1.15	1.15	1.00	R00r3	1019	1155.2	1.13	1.56	1.05	0.67
S10r1	872	871.4	1.00	1.34	1.37	1.02	R10r3	-	-	-	-	-	-
S20r1	883	925.1	1.05	1.76	1.64	0.93	R20r3	1331	1360.6	1.02	1.69	1.69	1.00
S00r3	731	777.8	1.06	1.01	1.06	1.05	C00	682	655.7	0.96	1.02	1.04	1.02
S10r3	846	868.5	1.03	3.27	1.45	0.44	C10	1013	913.2	0.90	4.14	10.0	2.42
S20r3	1049	991.3	0.94	5.23	6.00	1.15	C20	1560	1337.3	0.86	8.00	10.0	1.25
									Média geral:	0.99			1.08

(a) ratio between numerical and experimental results, colors indicate whether the ratio was conservative (green) or against security (red).

In Fig. 5, the compression stresses are shown on the upper surfaces of the columns reinforced with two layers of CFRP. Comparing the columns S20r1 and S20r3, it can be seen that the column with a greater rounding radius achieved greater compression stresses and, therefore, a greater resistance gain. In the prismatic sections, it is noted that, in the rounded corners, the magnitude of the compressive stresses is greater, while in the circular section a uniform distribution of pensions is observed throughout the period of the cross section.

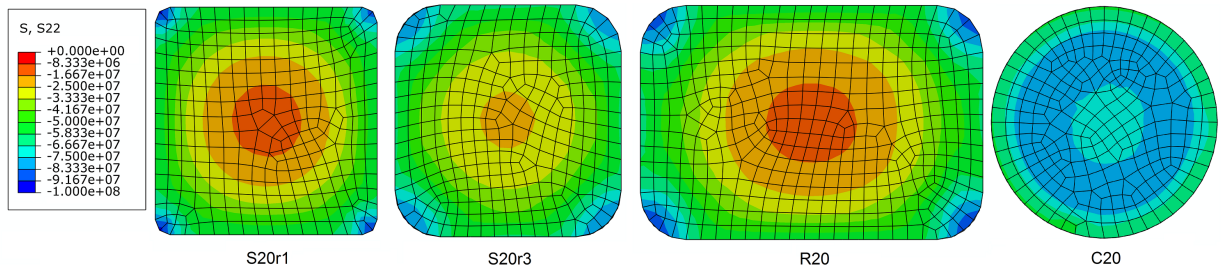

Figure 5. Compression stress distribution in the cross sections of the columns (values in Pa).

The application of different numbers of reinforcement layers allows a gradual increase of the axial compression strength in all tested and modeled columns compared to columns without reinforcement. Analyzing Fig. 6, the two-layer reinforcement proved to be the most efficient for all sections, with the circular section showing the best containment efficiency, reaching twice its resistant capacity.

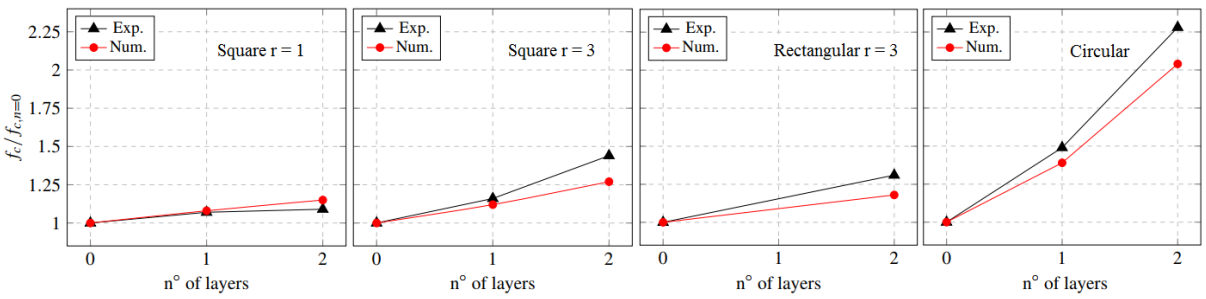

Figure 6. Influence of the number of CFRP layers

6 Conclusions

The finite element numerical modeling using the CDP proved to be capable of representing the concrete confinement mechanism for different cross sections of columns. However, it is necessary to calibrate some input parameters of the model so that the numerical results are similar to those of reality.

It was possible to observe that the increase in the rounding radius of the square column, led to a higher index of confinement, demonstrating that the effectiveness of the reinforcement is greater in the curved sections. In the circular column, the formation of the membrane effect is observed throughout the cross section, allowing the lateral restriction pressure of the reinforcement to be distributed evenly.

It is also concluded that the external reinforcement method with CFRP guarantees an increase in axial strength in concrete columns when subjected to centered compression. However, this efficiency is proven for a horizontal orientation of the carbon fibers, further research can be carried out on the use of different angles of application of the reinforcement in an attempt to optimize the structural performance of the columns.

Acknowledgements. The authors would like to thank the Cearense Foundation for Support for Scientific and Technological Development (FUNCAP) for the financial support for the development of this research.

Authorship statement. The authors hereby confirm that they are the sole liable persons responsible for the authorship of this work, and that all material that has been herein included as part of the present paper is either the property (and authorship) of the authors, or has the permission of the owners to be included here.

References

[1] Barros, J. A. & Ferreira, D. R., 2008. Assessing the efficiency of CFRP discrete confinement systems for concrete cylinders. *Journal of Composites for Construction*, vol. 12, n. 2, pp. 134–148.

[2] Wu, Y.-F. & Wei, Y.-Y., 2010. Effect of cross-sectional aspect ratio on the strength of CFRP-confined rectangular concrete columns. *Engineering Structures*, vol. 32, n. 1, pp. 32–45.

[3] Gajdošová, K. & Bilčík, J., 2011. Slender reinforced concrete columns strengthened with fibre reinforced polymers. *Slovak Journal of Civil Engineering*, vol. XIX, n. 2.

[4] Rahai, A. & Akbarpour, H., 2014. Experimental investigation on rectangular RC columns strengthened with CFRP composites under axial load and biaxial bending. *Composite Structures*, vol. 108, pp. 538–546.

[5] Oliveira, D. S. & Carrazedo, R., 2019. Numerical modeling of circular, square and rectangular concrete columns wrapped with FRP under concentric and eccentric load. *Revista IBRACON de Estruturas e Materiais*, vol. 12, n. 3, pp. 518–550.

[6] Raza, S., Khan, M. K. I., Menegon, S. J., Tsang, H.-H., & Wilson, J. L., 2019. Strengthening and repair of reinforced concrete columns by jacketing: State-of-the-art review. *Sustainability*, vol. 11, n. 11, pp. 3208.

[7] ACI, 2017. *440.2R-17: Guide for the design and construction of externally bonded FRP systems for strengthening concrete structures*. ACI Committee 440, Farmington Hills, Michigan, USA.

[8] Oliveira, D. S. & Carrazedo, R., 2016. Reforço em pilares retangulares de concreto com prf e tirantes de aço. *Revista Concreto e Construção*, vol. 44, n. 82, pp. 75–80.

[9] Sudano, A. L., 2010. *Desenvolvimento de estratégias híbridas de reforço de pilares de concreto armado por encamisamento com compósitos de alto desempenho*. Doutorado, Escola de Engenharia de São Carlos da Universidade de São Paulo, São Carlos.

[10] Machado, A. D. P., 2002. Reforço de estruturas de concreto armado com fibras de carbono: características, dimensionamento e aplicação. *Revista PINI*, pp. 282.

[11] Carneiro, L. A. V., 2004. *Reforço de vigas e pilares de concreto com materiais compósitos de resina e fibras*. Doutorado, COOPE/UFRJ, Rio de Janeiro, Brasil.

[12] Lubliner, J., Oliver, J., Oller, S., & Oñate, E., 1989. A plastic-damage model for concrete. *International Journal of Solids and Structures*, vol. 25, n. 3, pp. 299–326.

[13] Carrazedo, R., 2005. *Mecanismos de confinamento em pilares de concreto encamisados com polímeros reforçados com fibras submetidos à flexo- compressão*. Doutorado, Escola de Engenharia de São Carlos, Universidade de São Paulo, São Paulo.

[14] CEB-FIP, 1993. *Model Code 1990*. Thomas Telford, Lausanne, Switzerland.

[15] Mansur, M. A., Chin, M. S., & Wee, T. H., 1999. Stress-strain relationship of high-strength fiber concrete in compression. *Journal of Materials in Civil Engineering*, vol. 11, n. 1, pp. 21–29.

[16] Birtel, V. & Mark, P., 2006. Parameterised finite element modelling of RC beam shear failure. pp. 95–108.